Journal of Magnetics 5(4), 111-115 (2000)

Structural and Magnetic Properties of Co-Mn Ferrite Prepared by a Sol-gel Method

Woo Chul Kim, Young Suk Yi and Chul Sung Kim*

Department of Physics, Kookmin University, Seoul 136-702, Korea

(Received 25 July 2000)

Ultrafine $Co_{0.9}Mn_{0.1}Fe_2O_4$ powders have been fabricated by a sol-gel method. Structural and magnetic properties of the powders were investigated by x-ray diffractometry, transmission electron microscopy (TEM), Mössbauer spectroscopy, and vibrating sample magnetometry (VSM). Co-Mn ferrite powders that were fired at and above 773 K contained only a single spinel phase and behaved ferrimagnetically. Powders fired at 673 and 723 K had a spinel structure and were mixed paramagnetic and ferrimagnetic in nature. The magnetic behavior of Co-Mn ferrite powders fired at and above 873 K showed that an increase of the firing temperature yielded a decrease in the coercivity and an increase in the saturation magnetization. The maximum saturation magnetization and coercivity of Co-Mn ferrite powders were 66.7 emu/g and 1523 Oe, respectively. Mössbauer spectra of the powder fired at 923 K were taken at various temperatures ranging from 13 to 850 K. The iron ions at both *A* (tetrahedral) and *B* (octahedral) sites were found to be in ferric high-spin states. The Néel temperature T_N was found to be 850 ± 2 K. Debye temperatures for *A* and *B* sites were found to be Θ_A = 757 ± 5 K and Θ_B = 282 ± 5 K, respectively.

1. Introduction

The preparation and characterization of nano-crystalline ferrite powders have been studied extensively in recent years [1-3]. Ferrites are well known as magnetic compounds that have been studied for applications in microwave devices and as magnetic recording media using their novel physical properties [4, 5]. Cobalt ferrite, $CoFe_2O_4$, is a well-known magnetic material which has been studied in detail due to its high coercivity (5400 Oe) and moderate saturation magnetization (about 80 emu/g) as well as its remarkable chemical stability and mechanical hardness [6]. For use as high-density magnetic recording materials, the particles size of ferrite particles must be < 10 nm to avoid the exchange interaction between neighboring particles [7]. As the particle size becomes smaller than the critical size needed to keep satisfactory magnetic properties, the magnetization direction of the ultrafine ferrite powder is not fixed as in large crystals, but fluctuates spontaneously. Solution routes are commonly used to fabricate ultrafine powders, rather than solid-state reaction processes. One of the solution routes is the sol-gel method, which is known as a technique for low temperature synthesis of glass, ceramic, and other materials. One of the advantages of using the sol-gel method is the lower annealing temperature that enables smaller particle sizes to grow, e.g. nano-crystalline particles. Recently, sol-gel methods for the growth of ultrafine cobalt ferrite and barium ferrite powders have been investigated [8, 9]; however, ultrafine cobalt-manganese ferrite particles have not yet been investigated to a great extent.

*E-mail: cskim@phys.kookmin.ac.kr

2. Experiment

In this study, a sol-gel procedure was used for the growth of ultrafine Co-Mn ferrite powders and their structural and magnetic properties were characterized using x-ray diffraction, transmission electron microscopy (TEM), Mössbauer spectroscopy, and vibrating sample magnetometry (VSM). X-ray diffraction and TEM measurements provide information about the formation of phases, the crystallization temperature, and particle sizes. Mössbauer spectroscopy measurements were used to identify magnetic phases and magnetic properties of ultrafine powders. VSM measurements gave the saturation magnetization and coercivities of the Co-Mn ferrite powders as a function of firing temperature.

Ultrafine Co-Mn ferrite powders were synthesized by a sol-gel method. A block diagram outlining the preparation process for $Co_{0.9}Mn_{0.1}Fe_2O_4$ ferrite powder is shown in Fig. 1. Weighed amounts of $Co(CH_3CO_2)_2 \cdot 4H_2O$, $Mn(CH_3CO_2)_2 \cdot 4H_2O$, and $Fe(NO_3)_3 \cdot 9H_2O$ were first dissolved in 2-methoxyethanol (2-MOE) and water for 30 min using an ultrasonic cleaner. The solution was refluxed at 343 K for 12 h to allow gel formation and then dried at 373

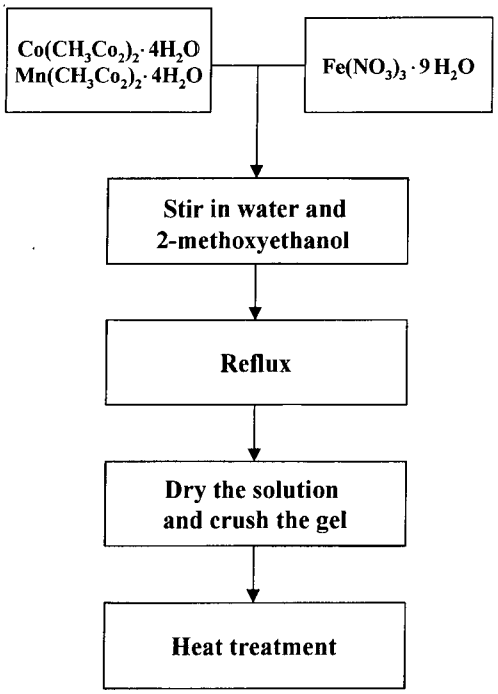

Fig. 1. Preparation process for the $Co_{0.9}Mn_{0.1}Fe_2O_4$ ferrite powder.

K in a dry oven for 24 h. The dried powder was ground and fired at various temperatures for 6 h in air. X-ray diffraction patterns of the samples were obtained with Cu $K\alpha$ radiation. The Mössbauer spectra were recorded using a conventional Mössbauer spectrometer of the electromechanical type [10] with a 30-mCi source in a Rh matrix.

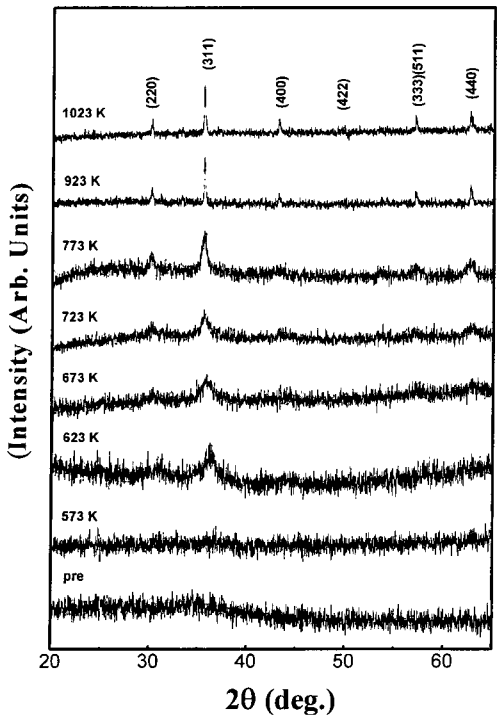

Fig. 2. Changes in the x-ray diffraction spectra of $Co_{0.9}Mn_{0.1}Fe_2O_4$ powders at various firing temperatures.

3. Result and Discussion

X-ray diffraction patterns of $Co_{0.9}Mn_{0.1}Fe_2O_4$ powders fired at various temperatures are shown in Fig. 2. All peaks of Co-Mn ferrite powders fired at and above 673 K are consistent with those of a typical spinel structure of a cobalt ferrite prepared by a conventional solid-state reaction [11]. However, the diffraction peaks for the powder fired at 673 K are fairly broad, indicating that the sample consists of quite fine crystallites. The line broadening for the other samples decreases with increase of the firing temperature corresponding to, the growth of larger particles of Co-Mn ferrite powders. Figure 3 shows TEM micrographs of the Co-Mn ferrite powders fired at 573 and 923 K. Particles of both samples are spherical in shape and have average particle size of 15 and 92 nm.

Mössbauer absorption spectra measured at room temperature for $Co_{0.9}Mn_{0.1}Fe_2O_4$ powders fired at different temperatures are shown in Fig. 4. Spectra of all samples fired at and above 773 K are fitted with two six-line subpatterns that are assigned to *A* ions in tetrahedral sites and *B* ions in octahedral sites of a typical spinel crystal structure. However, the spectrum for the samples fired at 673 and 723 K consists of two six-line subspectra and a doublet. It is sug-

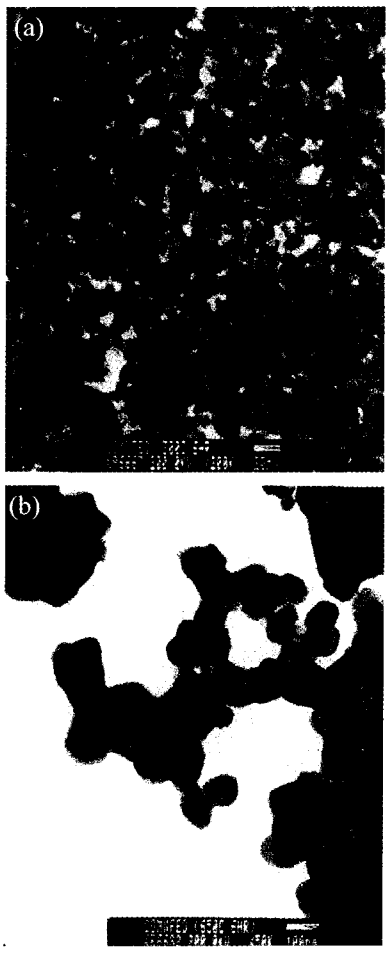

Fig. 3. Transmission electron microscopy (TEM) images of $Co_{0.9}Mn_{0.1}Fe_2O_4$ powders fired at 573 (a) and 923 K (b).

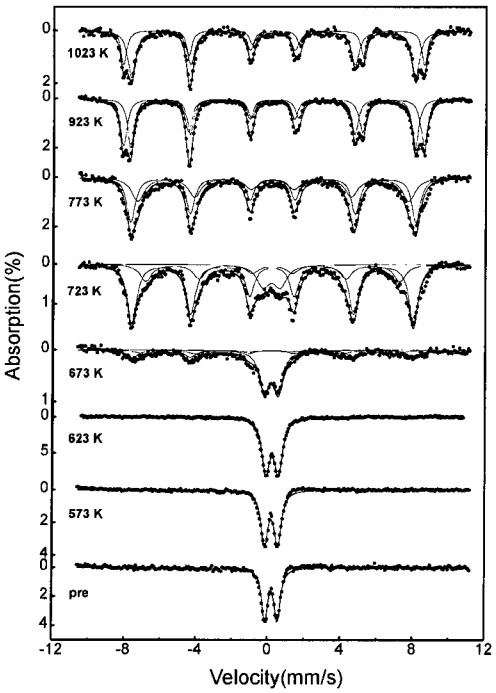

Fig. 4. Room-temperature Mössbauer spectra of $Co_{0.9}Mn_{0.1}Fe_2O_4$ at various firing temperatures.

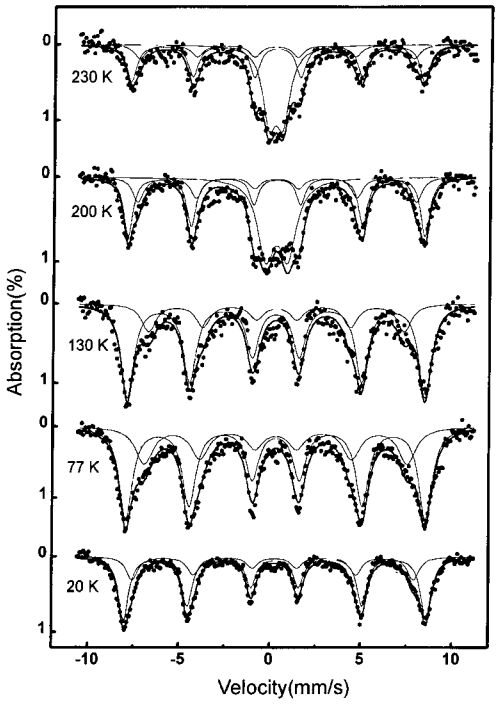

Fig. 5. Mössbauer spectra recorded at various temperatures of $Co_{0.9}Mn_{0.1}Fe_2O_4$ fired at 673 K.

gested that the samples fired at 673 and 723 K are both paramagnetic and ferrimagnetic in nature. In case of the sample fired at 673 K, 32% of the powder has particle too small to maintain the ferrimagnetic properties at room temperature and the remaining portion has a partice size large enough to become ferrimagnetic. The ratio of the two magnetic phases is based on the calculated absorption ratio of the two subspectra. The Mössbauer spectra measured at room temperature for the powder fired at 573 and 623 K, as shown in Fig. 4, are attributable to Fe ions in the superparamagnetic state in $Co_{0.9}Mn_{0.1}Fe_2O_4$ powders. That is, most of the Co-Mn ferrite particles fired at 573 and 623 K are too small to become ferrimagnetic.

Figure 5 shows the Mössbauer spectra of the sample fired at 673 K, taken at various temperatures. The change in the spectrum is typical for superparamagnetic materials as the measuring temperature decreases. These Mössbauer results are similar to those obtained by Grigorova *et al.* [12]. The spectra recorded at and below 130 K are fitted with two six-line subpatterns. The broad absorption lines of the two subspectra are related to the relaxation phenomena. When the measuring temperature is lowered, the relaxation time to maintain the ferrimagnetic property becomes larger so that some of the superparamagnetic Co-Mn ferrite particles become ferrimagnetic [13].

Figure 6 shows the Mössbauer spectra of the sample fired at 923 K taken at various temperatures. The spectra are composed of two six-line hyperfine patterns, *A* and *B*. Just above the Néel temperature of $T_N = 850 \pm 2$ K, the Mössbauer spectrum becomes a sharp doublet. Using a least-squares computer program, two sets of six Lorentzian lines

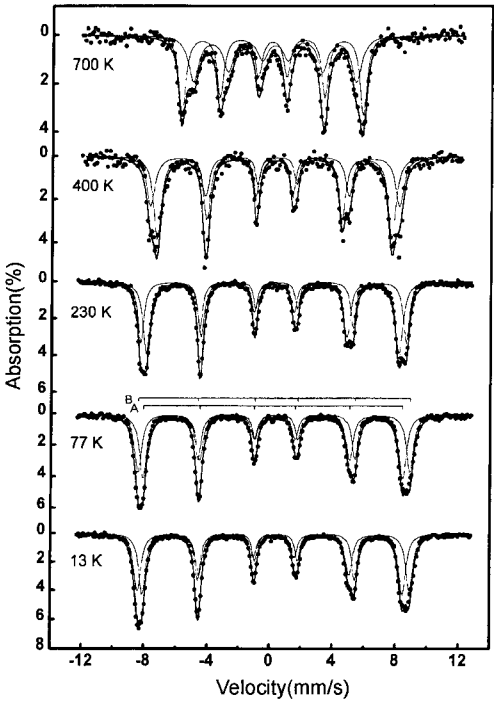

Fig. 6. Mössbauer spectra recorded at various temperatures of $Co_{0.9}Mn_{0.1}Fe_2O_4$ fired at 923 K.

were fitted to the Mössbauer spectra under the well-known restraints [14], which are valid when the quadrupole interaction is much weaker than the magnetic hyperfine interaction. The results of the computer analysis are presented in Table 1. The isomer shift values at room temperature for the *A* and *B* patterns were found to be 0.14 ± 0.01 mm/s and 0.24 ± 0.01 mm/s relative to Fe metal, respectively, which

Table 1. Magnetic hyperfine field (H_{hf}), quadrupole shift (ΔE_Q), and isomer shift (δ) for the tetrahedral (A) and the octahedral (B) sites at various temperatures T for $Co_{0.9}Mn_{0.1}Fe_2O_4$ annealed at 923 K. δ is relative to the iron metal

T (K)	H_{hf} (kOe)		ΔE_Q (mm/s)		δ (mm/s)	
	B	A	B	A	B	A
13	538	514	-0.09	-0.05	0.33	0.23
77	537	513	-0.08	-0.06	0.32	0.23
295	514	486	-0.08	-0.01	0.24	0.14
500	468	433	-0.07	0.02	0.20	0.11

were consistent with a high-spin Fe charge state [15]. The smaller value of the A site isomer shift was due to a larger covalency at the A site. The magnetic hyperfine field values at 13 K are 514 and 538 kOe for the A and B patterns, respectively, which are typical values for ferric ions. Plots of reduced magnetic hyperfine fields $H_{hf}(T)/H_{hf}(0)$ against reduced temperature T/T_N for A and B sites of $Co_{0.9}Mn_{0.1}Fe_2O_4$ are given in Fig. 7 along with the Brillouin curve $B(S)$ for $S = 5/2$. From these plots, it is seen that the magnetic fields (within the experimental error) are proportional to the sublattice magnetization. Figure 8 shows the temperature dependence of the resonant absorption area. The Debye model gives the following expression for the recoil-free fraction [16].

$$f = \exp\left[-\frac{3E_R}{2k_B\Theta}\left(1 + \frac{4T^2}{\Theta^2}\int_0^{\Theta/T}\frac{x\,dx}{e^x - 1}\right)\right], \quad (1)$$

where E_R is the recoil energy of ^{57}Fe for the 14.4 keV gamma ray. Θ and k_B represent the Debye temperature and Boltzman constant, respectively. The Debye temperature for each site can be calculated from the temperature dependence of the resonant absorption area of each subspectrum at low temperatures. The calculated Debye temperatures of the A and B sites were $\Theta_A = 757 \pm 5$ K and $\Theta_B = 282 \pm 5$ K.

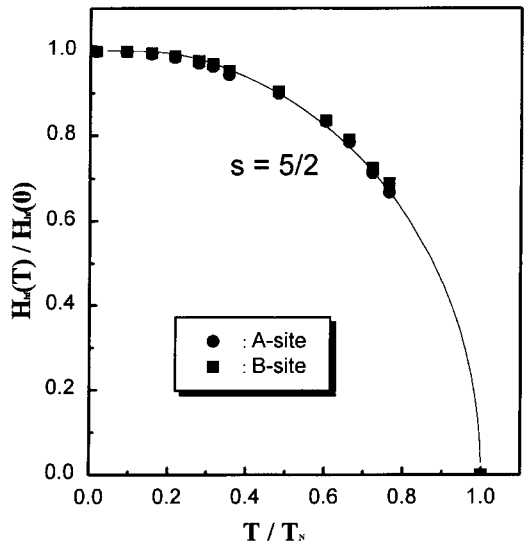

Fig. 7. Reduced magnetic hyperfine fields $H_{hf}(T)/H_{hf}(0)$ against reduced temperature T/T_N for A and B sites of $Co_{0.9}Mn_{0.1}Fe_2O_4$ fired at 923 K. Points marked are the experimental values. The full curve is the Brillouin curve for $S = 5/2$.

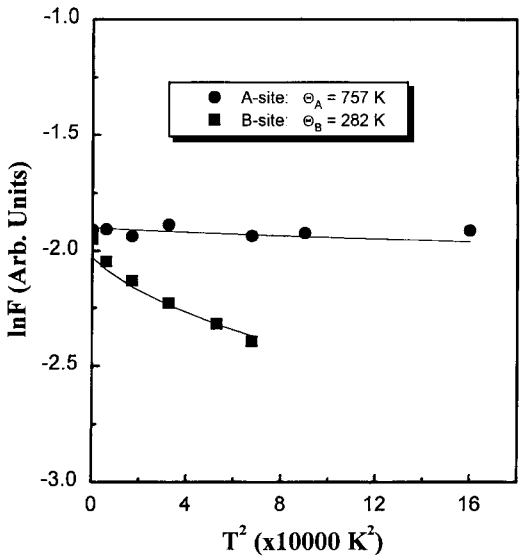

Fig. 8. Natural logarithm of the absorption area ln F *vs.* T^2 for the A and B subspectra of $Co_{0.9}Mn_{0.1}Fe_2O_4$ fired at 923 K.

The magnetic properties of annealed powders have been determined at room temperature using a vibrating sample magnetometer. Figure 9 shows the firing temperature dependence of saturation magnetization and coercivity at a maximum field of 15 kOe. The saturation magnetization increases drastically with firing temperature. However, the coercivity decreases when the annealing temperature is higher than 873 K. This magnetic behavior is related to the variation of the particle size. The samples fired at 573 and 623 K show only a small saturation magnetization. With the Mössbauer spectroscopy measurement, it is known that most of the Co-Mn ferrite particles have particle sizes

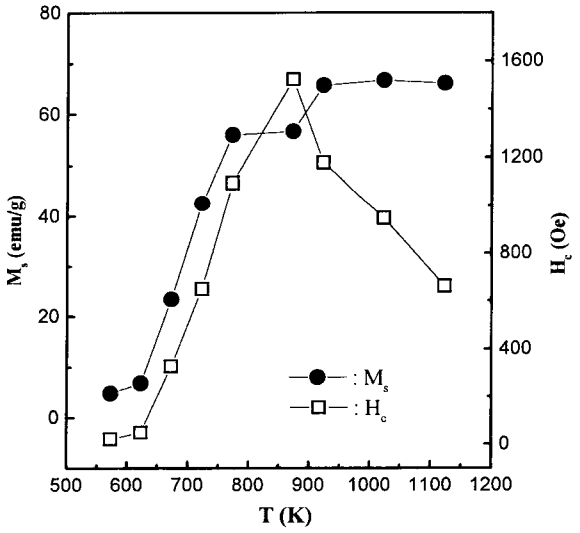

Fig. 9. Changes of saturation magnetization and coercivitis for $Co_{0.9}Mn_{0.1}Fe_2O_4$ powders as a function of firing temperature.

smaller than the critical size to maintain their magnetic properties. The maximum saturation magnetization and coercivity of Co-Mn ferrite powders are 66.7 emu/g and 1523 Oe measured in a maximum external field of 15 kOe. However, these two values are not of faired at the same exactly the same firing temperature.

Acknowledgments

This work was supported by the NON-Directed Research Fund through Korea Research Foundation (1997-001-D00145) and by the Brain Korea 21 Program.

References

[1] C. S. Kim, Y. S. Yi, K. T. Park, H. Namgung, and J. G. Lee, J. Appl. Phys. **85**, 5223 (1999).
[2] W. C. Kim, S. W. Lee, S. J. Kim, and C. S. Kim, J. Magn. Magn. Mater. **215-216**, 217 (2000).
[3] V. Blaskov, V. Petkov, V. Rusanov, L. M. Martinez, B. Martinez, J. S. Munoz, and Mikhov, J. Magn. Magn. Mater. **162**, 331 (1996).
[4] C. S. Kim, S. W. Lee, S. I. Park, J. Y. Park, and Y. J. Oh, J. Appl. Phys. **79**, 5428 (1996).
[5] S. N. Okuno, S. Hashimoto, and K. Inomata, J. Appl. Phys. **71**, 5926 (1992).
[6] T. Kodama, Y. Kitayama, M. Tsuji, and Y. Tamaura, J. Magn. Soc. Jpn. **20**, 305 (1996).
[7] E. S. Murdock, IEEE Trans. Magn. **28**, 3078 (1992).
[8] V. K. Sankaranarayana, Q. A. Pankhurst, D. P. E. Dickson, and C. E. Johnson, J. Magn. Magn. Mater. **125**, 199 (1993).
[9] J. G. Lee, J. Y. Park, and C. S. Kim, J. Mater. Sci. **33**, 3965 (1998).
[10] H. N. Ok, K. S. Baek, E. C. Kim, and C. S. Kim, Phys. Rev. B **48**, 3212 (1993).
[11] G. A. Sawatzky, F. Vander Woude, and A. H. Morrish, Phys. Rev. **187**, 747 (1969).
[12] M. Grigorova, H. J. Blythe, V. Blaskov, V. Rusanov, V. Masheva, D. Nihtianova, L. M. Martinez, J. S. Munoz, and M. Mikhov, J. Magn. Magn. Mater. **183**, 163 (1998).
[13] K. S. Baek, H. N. Ok, and J. C. Sur, Phys. Rev. B **39**, 2800 (1989).
[14] C. S. Kim, H. M. Ko, W. H. Lee, and C. S. Lee, J. Appl. Phys. **73**, 6298 (1993).
[15] S. W. Lee, D. H. Kim, S. R. Hong, S. J. Kim, W. C. Kim, S. B. Kim, and C. S. Kim, IEEE Trans. Magn. **35**, 3418 (1999).
[16] R. L. Mössbauer and W. H. Wiedermann, Z. Phys. **159**, 33 (1960); B. Kaufman and H. J. Lipkin, Ann. Phys. (N.Y.) **18**, 294 (1962).